BJP BRITISH JOURNAL OF PHARMACOLOGY

BPS BRITISH PHARMACOLOGICAL SOCIETY

British Journal of Pharmacology (2010), 161, 1219–1237

0007-1188/10
www.brjpharmacol.org

Themed Section: Analytical Receptor Pharmacology in Drug Discovery

REVIEW

Ligand binding assays at equilibrium: validation and interpretation

Edward C. Hulme[1] and Mike A. Trevethick[2]

[1]*Division of Physical Biochemistry, MRC National Institute for Medical Research, Mill Hill, London, UK, and* [2]*Discovery Biology, Pfizer Global R&D, Sandwich, Kent, UK*

The focus of this review paper is factors affecting data interpretation in ligand binding assays under equilibrium conditions. Protocols for determining K_d (the equilibrium dissociation constant) and K_{dA} (the equilibrium inhibitor constant) for receptor ligands are discussed. The basic theory describing the interaction of a radiotracer and an unlabelled competitor ligand with a receptor is developed. Inappropriate experimental design may result in ligand depletion and non-attainment of equilibrium, distorting the calculation of K_d and K_{dA}. Strategies, both theoretical and practical, will be given to avoid and correct such errors, thus leading to the determination of reliable values for these constants. In determining K_{dA} from competition binding studies, two additional concepts are discussed. First, the necessity to measure an adequate specific binding signal from the bound radiotracer ligand limits the range of affinity constants that can be measured: a particular set of assay conditions may lead to an upper limit on the apparent affinity of unlabelled ligands. Second, an extension of the basic assay methodology can indicate whether the interaction between the tracer and a test ligand is mediated by a competitive or an allosteric mechanism. Finally, the review ends with a discussion of two factors that are often overlooked: buffer composition and the temperature at which the assay is conducted, and the impact these can have on affinity measurements and the understanding of drug interactions.
British Journal of Pharmacology (2010) **161,** 1219–1237; doi:10.1111/j.1476-5381.2009.00604.x; published online 2 February 2010

This article is part of a themed section on Analytical Receptor Pharmacology in Drug Discovery. To view the other articles in this section visit http://dx.doi.org/10.1111/bph.2010.161.issue-6

Keywords: receptor; GPCR; equilibrium; kinetics; radioligand; ligand binding assay; antagonist; K_d; K_{dA}; competitive; depletion; allosteric; buffer; entropy; enthalpy; temperature

Abbreviations: BPS, British Pharmacological Society; GPCR, G protein-coupled receptor; mAChR, muscarinic acetylcholine receptor; mCi, millicurie; NMS, (–) *N*-methyl scopolamine; QNB, (–)-3-quinuclidinyl benzilate

Introduction

Two of the outstanding aims of binding studies on pharmacological receptors are to: (i) obtain reliable estimates of the affinities of selected ligands for the receptor of interest together with their associated errors; and (ii) analyse the mechanism of interaction of ligands with the receptor alone, and in combination. Such information provides an important contribution to drug screening and development programmes. The primary focus of this paper is the determination of reliable values for the binding constants that govern receptor–ligand equilibria *in vitro*. The kinetic processes governing ligand association and dissociation will be considered to the extent that they are needed to understand equilibrium binding experiments, to formulate mathematical models for their analysis and to avoid systematic errors in their performance. The interesting and important role of the dissociation rate constant, in particular, in determining ligand selectivity, efficacy and duration under non-equilibrium conditions *in vivo* has been addressed in excellent recent reviews (Copeland *et al.*, 2006; Swinney (2009). Receptor nomenclature is written according to the recommendations published in the British Pharmacological Society Guide to Receptors and Channels (Alexander *et al.*, 2008).

Correspondence: Mike A. Trevethick, Discovery Biology, Pfizer Global R&D, Sandwich, Kent CT13 9NJ, UK. E-mail: mike.trevethick@pfizer.com; Edward C Hulme, Division of Physical Biochemistry, MRC National Institute for Medical Research, Mill Hill, London NW7 1AA, UK. E-mail: ehulme@nimr.mrc.ac.uk
Receptor nomenclature is written according to the recommendations published in the British Pharmacological Society *Guide to Receptors and Channels* (Alexander *et al.*, 2008).
Received 10 September 2009; revised 19 October 2009; accepted 29 October 2009

Principles of receptor binding assays

There are several stages in the development of a binding programme: initial choices, establishment of assay conditions, validation, application to novel ligands and quantitative

analysis of the resulting data to derive binding parameters for the ligands. These steps are overlapping, interactive and recursive. Nevertheless, a number of definite milestones need to be achieved.

Numerous publications have covered practical aspects of setting up a ligand binding assay (Hulme and Birdsall, 1992; Lazareno, 1998). We shall assume the use of a radiolabelled ligand, with rapid membrane filtration to separate bound from free ligand. However, the receptor preparation may also be immobilized on a Biacore surface plasmon resonance chip or on scintillation proximity beads (Glickman *et al.*, 2008), generating a signal from ligand binding without the need for a mechanical separation. Alternatively, binding may be monitored by a spectroscopic signal. General considerations for the development of ligand binding assays apply to these formats as well.

Fundamentally, three types of receptor binding experiments may be performed:

- Kinetic experiments, where the binding of one or more concentrations of radioligand is measured at an incrementing series of time points, and analysed to estimate association (k_{on}) and dissociation (k_{off}) rate constants.
- Saturation experiments, where binding of an increasing series of concentrations of a radioligand, L, is measured at equilibrium and analysed to determine its binding constant (affinity constant, K, or dissociation constant, K_d) and the concentration of specific binding sites for the radioligand (R_T); the experimentally determined estimate of R_T is usually designated B_{Max}.
- Competition/modulation experiments where the binding of one or more fixed concentrations of a radioligand is measured at equilibrium in the presence of an incrementing series of concentrations of a non-labelled compound, and the data analysed to determine the binding constant of the compound for the unliganded receptor, and the cooperativity between the compound and the radioligand for binding to the receptor. Classically, the equilibrium inhibitor constant K_i is calculated from such experiments using the Cheng–Prusoff transformation ($K_i = IC_{50}/(1 + [L]/K_{dL})$. In this paper, we usually use the designation A for an unlabelled ligand; in this case, it is the dissociation constant for A, K_{dA} that corresponds to K_i.

The experimental protocol for binding assays is (somewhat deceptively) straightforward: (i) make a preparation containing the receptor, for instance, a membrane fraction, that can be divided into aliquots; (ii) select a suitable labelled ligand; (iii) incubate aliquots of the receptor preparation with chosen concentrations of the labelled ligand for a defined time at a defined temperature in a defined buffer; (iv) measure the bound and (sometimes or) free ligand concentration; (v) repeat steps (iii) and (iv) with the addition of unlabelled ligands or modulating agents, as defined by the aims of the experiment; and (vi) analyse the data mathematically to extract quantitative estimates of rate constants, affinity constants and cooperativities.

It is easy to do binding experiments and obtain data. However, binding reactions, like gravitational interactions, are highly non-linear, and this can lead the unwary practitioner into artefacts and pitfalls. Non-equilibrium and ligand depletions are particular hazards, which can be exacerbated by undetected impurities in the ligands studied. They can lead to the inaccurate estimation of ligand binding constants. This can have important consequences if the values are used, for instance, for the calculation of receptor occupancies *in vivo*, for estimating the potencies of new compounds or for the comparison of structure–activity relationships.

The purpose of this review was to outline the basis of equilibrium binding studies. We focus on how to set up, verify and analyse receptor binding assays to obtain authentic results. We illustrate the theoretical considerations with a number of experimental examples. At the outset, we assume that a suitable receptor preparation is available, that a labelled tracer ligand has been synthesized for the receptor under study and that a test set of unlabelled competitor ligands with known pharmacology is available. Usually, the receptor preparation is a membrane suspension.

Theoretical foundations of receptor binding studies

In the following section, we outline the fundamental theory of ligand binding studies.

A basic understanding of the theory of receptor–ligand interactions is essential for the planning, execution, analysis and interpretation of binding experiments. This enables the practitioner to take a critical and discriminating stance, for instance, when choosing from the equations embedded in standard data analysis packages. As in all quantitative subjects, equations are power!

Saturation binding studies

At the level of the individual receptor molecule, ligand binding and dissociation are stochastic processes. An (imperfect) analogy is the uptake of glasses of wine by delegates at a BPS meeting reception. Within a certain time period, the thirsty delegate [unliganded receptor (R)] has a probability of acquiring a wine glass (ligand) that is proportional to the product of the density of glasses on the circulating trays [ligand concentration (L)] and the probability of productive encounter and capture (k_{on}; this is an example of a simple bimolecular association reaction). Having acquired a glass of wine, the delegate [now liganded receptor (RL)] then has a fixed probability (k_{off}) of relinquishing it within an equivalent period.

$$R + L \underset{k_{off}}{\overset{k_{on}}{\rightleftharpoons}} RL$$

After the elapse of a certain interval, an objective observer (probably drinking orange juice) will notice that although the state of individual delegates may fluctuate, the fraction of them holding glasses, as well as the total number of glasses held, builds up towards a steady state, which is maintained until the waiters clear the empty glasses away, and reluctantly, mono-exponentially, but eventually completely, they dissociate from the delegates' hands.

At the steady state, the rate of uptake is equal to the rate of release, $k_{on}[R][L] = k_{off}[RL]$, where $[R]$ and $[L]$ represent the free molar concentrations of receptor and ligand, and k_{on} and k_{off} are the association and dissociation rate constants (dimen-

sions concentration^{-1} time^{-1} and time^{-1} respectively). Here, the drinks reception analogy breaks down because, in the case of receptor equilibrium binding, the receptor and ligand remain unmodified after parting company. Furthermore, it is the binding event itself (the glass, not the contents!) that induces a conformational change in the receptor. In addition, the total concentration of receptors is conserved: $[R] + [RL] = [R_T]$, no further delegates enter and none leave for the bar! They are also assumed to be homogeneous (no preference for red over white) and equally accessible to ligand (no delegates trapped in crowds around posters).

Under these conditions, the steady state achieved represents the binding equilibrium between the receptor and the ligand, obeying the law of mass action:

$$\frac{[RL]}{[R][L]} = \frac{k_{on}}{k_{off}} = K$$

K, the equilibrium affinity constant, has dimensions of M^{-1}. As K (analogous to the thirst of the delegates) increases, so the concentration of the receptor–ligand complexes increases at the expense of the free species. Alternatively,

$$\frac{[R][L]}{[RL]} = \frac{k_{off}}{k_{on}} = K_d$$

defines the equilibrium dissociation constant, K_d, which is a measure of the tendency of the receptor–ligand complex to dissociate. This has dimensions of M. It is usually 10^{-9} M (1 nM) or lower for an interaction that is useful for radioligand binding studies. These expressions can be used interchangeably to calculate the concentration of the receptor–ligand complex as a function of the free ligand concentration. Thus, substituting the expression $[RL] = K[R][L]$ into the receptor conservation condition, we obtain $[R] + K[R][L] = [R_T]$ from which

$$[RL] = \frac{K[L][R_T]}{1 + K[L]} \quad (1a)$$

$$\text{Alternatively,} \quad [RL] = \frac{[L][R_T]}{[L] + K_d} \quad (1b)$$

Equation 1(a) and 1(b) are forms of the Langmuir isotherm, which describes the equilibrium binding of a single ligand species to a single uniform population of receptor binding sites.

- One-site binding shows a smooth (hyperbolic) saturable dependence of the concentration of the receptor–ligand complex on the free ligand concentration. An example of a saturation binding curve is given in Figure 1A.

The initial slope of the binding curve, at low ligand concentration ($[L] = 0.1 \times K_d$), is given by $K[R_T]$. The slope falls to 50% of its initial value when $[L] = K_d$, at which point 50% of the receptor population is occupied by ligand, so $[RL] = [R_T]/2$. When $[L] = 10 \times K_d$, the occupancy achieves 91% of its maximum value $[R_T]$. The experimental estimate of this maximum binding capacity is usually designated B_{Max}. A typical binding curve spans more than two orders of magnitude of ligand concentration.

- Saturation binding curves are frequently plotted as a function of $\log_{10}[L]$, often after normalization by division of the concentration of the receptor–ligand complex by the total estimated concentration of binding sites B_{Max} to yield an occupancy value P. In a simple case, this yields a sigmoid binding curve, which is symmetrical about $\log_{10}K_d$ (Figure 1B).
- When fitted with the Hill equation, $(P = (K[L])^{nH}/(1 + (K[L])^{nH})$, simple one-site binding curves have a slope factor (n_H) of 1.0.

One-site occupancy–concentration curves with different values of K_d lie parallel to one another, with the same sigmoid shape, when plotted semi-logarithmically against ligand concentration, but occupy different positions on the log concentration axis.

- pK_d, defined as $-\log_{10}K_d$ ($= \log_{10}K$) is a parameter of fundamental importance for the comparison of ligand affinities and selectivities, and for the prediction of drug concentrations that are efficacious *in vivo*. These are often about $3 \times K_d$.

The accurate determination of the pK_d of the radioligand is also essential for the accurate determination of the binding parameters (pK_d and cooperativity) of unlabelled drugs by the modulation of tracer ligand binding, as discussed below.

- Algorithms for the analysis of experimental equilibrium binding data should be formulated to produce estimates of pK_d and their associated errors as an output. This is because pK_d is normally distributed, but K_d is not.

Time-course of binding and dissociation

The use of equation 1 for the analysis of data requires: (i) that the binding reaction has achieved equilibrium; and (ii) that the concentration of free ligand, $[L]$, in equilibrium with the receptor–ligand complex can be measured or estimated. Factors affecting the rate of equilibration will be discussed first.

The rate of change of the concentration of the receptor–ligand complex is equal to the difference between its rate of formation and dissociation, so $d[RL]/dt = k_{on}.[R][L] - k_{off}.[RL]$. For a simple bimolecular association–dissociation reaction, the time-course is described by a single exponential process.

$$[RL] = ([RL_0] - [RL_{eq}])e^{-(k_{on}[L] + k_{off})t} + [RL_{eq}] \quad (2)$$

$[RL_0]$ is zero in an association experiment initiated by the addition of ligand to receptor. In this case, the concentration of the receptor–ligand complex increases smoothly and asymptotically towards its final equilibrium value $[RL_{eq}]$.

- The observed rate constant of the association reaction, $k_{obs} = k_{on}.[L] + k_{off}$, increases with the free ligand concentration. An experimental example is shown in Figure 2A. It is slowest when limited by the dissociation rate constant at low ligand concentrations.
- Replotting k_{obs} as a function of $[L]$ gives a straight line; k_{on} is determined by the slope as shown in Figure 2B. In favourable cases, k_{off} can be estimated from the y-intercept.

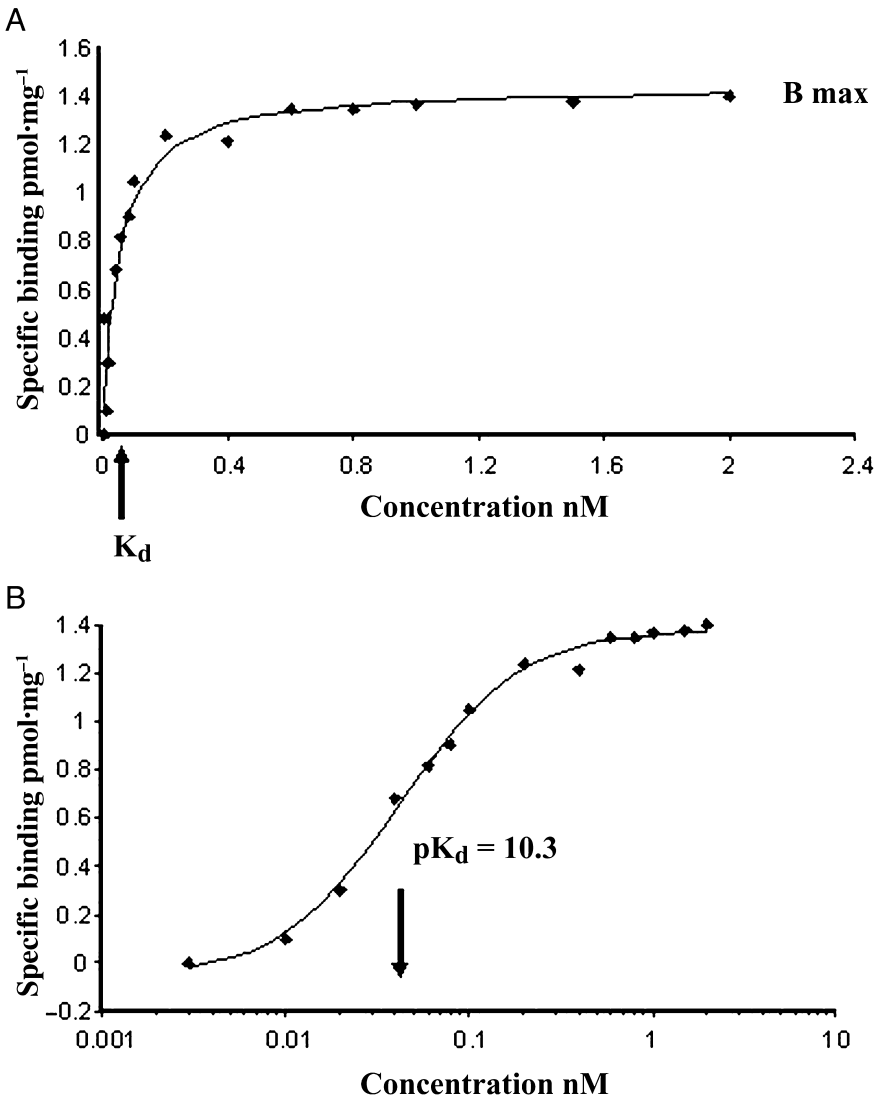

Figure 1 Saturation binding curve for a radioligand. Specific binding of [^{3}H]oxytropium to membranes from CHO cells expressing the human muscarinic M_3 receptor is shown. Radioligand depletion was 13% at the lowest concentration tested. The incubation time was 2 h at room temperature in 20 mM HEPES buffer, pH 7.4. Atropine was used to define non-specific binding. (A) Saturation binding curve plotted on a linear scale. The full line is the fit of equation 1b to the data. The estimated K_d was 0.05 nM, and the B_{Max} 1.4 pmol·mg^{-1} protein; (B) data from (A) replotted against log concentration (*x*-axis) to reveal the characteristic sigmoid concentration–response curve.

Rewriting $k_{obs} = k_{off}(1 + K[L]) = k_{off}(1 + [L]/K_d)$ emphasizes that the observed rate of equilibration depends on the ligand concentration in relation to the K_d; for instance, it will be ca. 10-fold faster at 90% receptor occupancy than at 10% receptor occupancy. At low occupancy, the equilibration rate is determined by k_{off}. The half-time of the equilibration reaction is given by $t_{1/2} = \log_e(2)/k_{obs} = 0.693/k_{obs}$. The time taken to attain 97% of the final equilibrium value is $5 \times t_{1/2}$. For instance, the muscarinic antagonist tiotropium has a K_d of 10 pM and a k_{off} of 0.0015 min^{-1} (Dowling and Charlton, 2006) giving a half-time of 462 min. Thus, if tiotropium is used at a concentration of 100 pM ($10 \times K_d$), the assay equilibrium time is ca. 210 min (3.5 h), but at 0.3 pM, this extends to ca. 2100 min (35 h).

- The use of an incubation time greater than $5 \times 0.693/k_{off} = 5 \times t_{1/2}$ for the dissociation reaction is a fail-safe assumption for ensuring equilibrium in binding studies with a single radioligand which has mono-exponential dissociation kinetics, provided that no competitors or modulators are also present.
- The determination of k_{off} is therefore an essential step in validating a radioligand binding assay.

This usually entails: (i) pre-labelling of the receptor to equilibrium with a concentration (e.g. $10 \times K_d$) of the radiolabelled tracer that provides high initial occupancy; and (ii) inducing its dissociation by the addition of a receptor-saturating concentration (e.g. $1000 \times K_d$) of an unlabelled competing ligand that prevents re-binding of the radioligand. The dissociation time-course is then analysed using an exponential function, $[RL] = [RL_0]e^{-k_{off}t}$. An experimental example is shown in Figure 2C; in this case, $t_{1/2}$ was 8.7 min, indicating that an incubation time of 43 min is sufficient to ensure equilibrium binding of the tracer ligand, irrespective of the starting conditions.

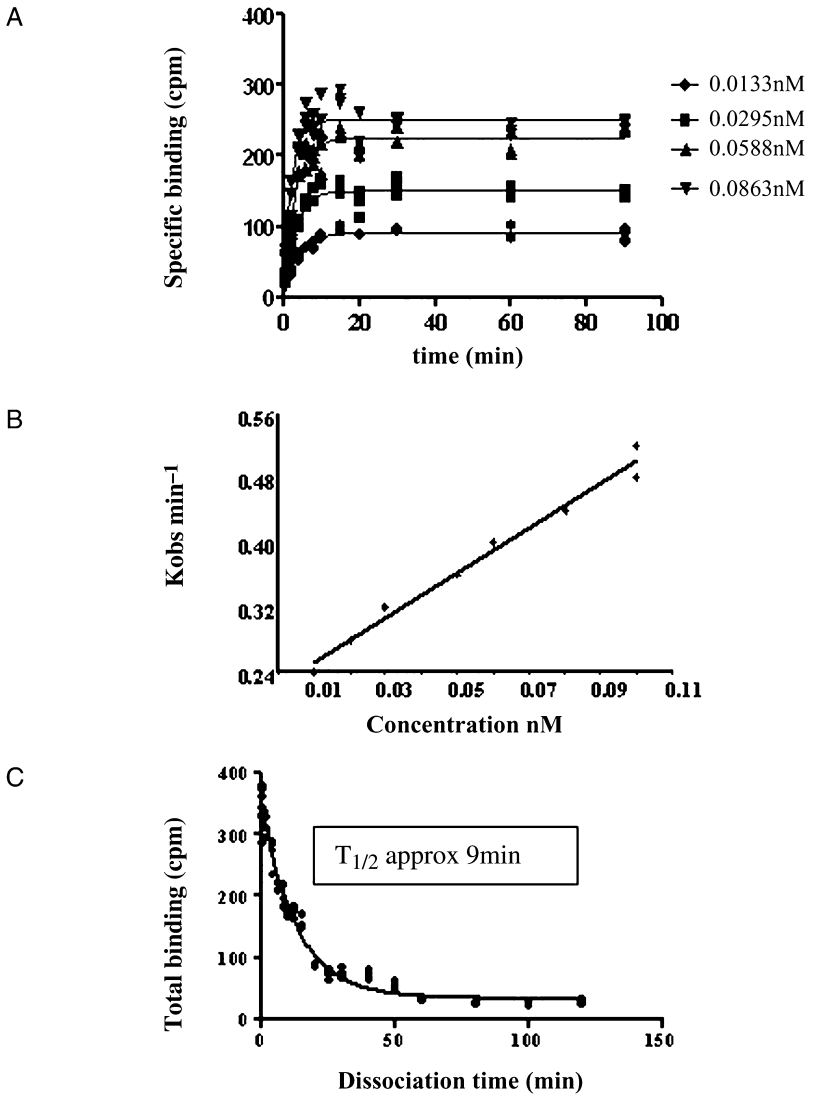

Figure 2 Kinetic studies of radioligand association and dissociation. Kinetic studies of the binding of [^{3}H]oxytropium to M_3 mAChRs: (A) association time-courses using several concentrations of oxytropium spanning the K_d; the full lines are fits to equation 2, giving values of k_{obs}, the apparent association rate constant; (B) determination of the association rate constant (k_{on}) from the fits shown in 2(A); k_{obs} was plotted against the concentration of oxytropium and the slope determined by linear regression, giving an estimate for k_{on} of 2.1×10^9 $M^{-1}{\cdot}min^{-1}$ (3.5×10^7 $M^{-1}{\cdot}s^{-1}$); (C) dissociation of oxytropium (0.3 nM) initiated with 10 μM atropine; the full line is the fit to a single exponential, with k_{off} 0.08 min^{-1}, corresponding to $t_{1/2}$ = 8.7 min. The ratio of k_{off}/k_{on} gives 3.8×10^{-11} M (0.038 nM) for the K_d, in good agreement with the value from the direct saturation study (Figure 1).

An example of a discrepancy between K_d calculated from saturation binding compared to kinetic analysis is demonstrated in a publication by Sullivan *et al.* (2006). These workers found that the K_d of [^{3}H]NBI 42 902 binding to membranes expressing the type 1 GnRH receptor determined in saturation binding studies with an incubation time of 2 h was 200 pM. However, radioligand dissociation experiments gave a half-time of 4 h, suggesting that an adequate incubation time in saturation binding studies would have been at least 20 h! Failure to attain equilibrium in the saturation binding studies led to an overestimated K_d. The true K_d, calculated from kinetic analysis (k_{off}/k_{on}), was 29 pM.

In more complicated cases, the dissociation time-course may fit to a sum of exponentials. This may indicate the induction of a conformational change in the receptor after the initial binding step, the reversal of which is rate limiting (Copeland *et al.*, 2006). In this instance, it is the half-time of the slowest process that should be used to calculate the equilibration time. Experimentally, k_{off} values are often strongly temperature sensitive, indicating an enthalpic contribution to the free energy of activation of the dissociation reaction. Because of this, they may be reduced, and the corresponding equilibration time increased by about 30-fold at 0°C compared to 30°C. In addition, k_{off} may be strongly influenced by buffer conditions. Therefore:

- The dissociation rate constant should always be determined under the conditions of the assay.

The effect of radioligand depletion on tracer association and equilibrium binding

The thirsty delegates at the BPS reception may be frustrated to find that the drinks tray, initially fully laden, has been emptied by other participants before it comes into reach; unfortunately, it is only in a utopian world that the waiters maintain a constant density of circulating wine glasses! Similarly, in a binding reaction, the total amount of ligand present is determined by the amount added at the outset, so that the free ligand concentration diminishes as the binding reaction proceeds, because the ligand, like the receptor, is subject to a conservation condition; $[L] + [RL] = [L_T]$, and $[L] = [L_T] - [RL]$. To account for this, the rate of change of receptor–ligand concentration must be amended and rewritten in terms of the total concentrations as follows:

$$d[RL]/dt = k_{on}([R_T] - [RL])([L_T] - [RL]) - k_{off}[RL]$$

At equilibrium, it follows that the quadratic equation

$$[RL]^2 - [RL]([R_T] + [L_T] + K_d) + [R_T][L_T] = 0$$

governs the relationship between the concentration of receptor–ligand complex, the total concentrations of receptor and ligand present in the assay and the K_d. Note that there is no formal distinction between receptor and ligand in these equations, or in the solution, which the frustrated delegate will undoubtedly recollect, from high school algebra, is:

$$[RL] = \frac{([R_T] + [L_T] + K_d) - \sqrt{([R_T] + [L_T] + K_d)\,\wedge 2 - 4[R_T][L_T]}}{2} \quad (3)$$

- Equation 3, after the addition of a term to describe non-specific binding (see below), is the appropriate equation to analyse radioligand saturation data in terms of the total concentration of ligand added to the assays by the experimenter. K_d is written as 10^{-pKd} within the curve-fitting algorithm, so that the optimized parameter is pK_d. Ligand and receptor concentrations, and K_d, must be scaled to reasonable units (e.g. nM) during fitting. A K_d of 1 nM gives pK_d = 0 on a nM scale.

The formula describing ligand association also requires correction, taking the form

$$[RL] = \frac{a \cdot b(e^{(a-b)k_{on}t} - 1)}{(ae^{(a-b)k_{on}t} - b)} \quad (4)$$

where $a = [RL_{eq}]$, the level of equilibrium binding calculated from equation 3 and $b = [R_T][L_T]/[RL_{eq}]$. This expression, known as the integrated rate equation, again does not discriminate between the binding partners, the delegates and the glasses! In accord with real-life experience, the plateau represented by equation 4 is lower, and reached sooner, than that from equation 2 (Hulme and Birdsall, 1992). It should be noted that this does not affect the determination of the all-important value of k_{off} initiated by the addition of a receptor-saturating concentration of a non-labelled competitor.

- The reduction of the free ligand concentration as a direct result of receptor binding is called ligand depletion, δ. Assuming that non-receptor binding can be ignored, δ is defined as $[RL]/[L_T]$.

Radioligand depletion is most pronounced at the lowest ligand concentrations, when its equilibrium value may be approximated by $[R_T]/(K_d + [R_T])$.

- The total concentration of ligand giving 50% receptor occupancy (where the free ligand $[L] = K_d$) is designated EC_{50}. Application of the conservation condition for ligand shows directly that $EC_{50} = K_d + [R_T]/2$.

$\delta = [R_T]/(2K_d + [R_T])$ at the EC_{50}, illustrating how ligand depletion diminishes as receptor saturation increases.

- Ideally, in ligand binding studies, radioligand depletion should be held to less than 10%; this means that $[R_T] < 0.1\ K_d$. Under these conditions, EC_{50} exceeds K_d by at most 5%. The exact equation 3 is similarly approximated by equation 1b, with $[L] = [L_T]$. The use of the exact equation is still recommended for data analysis.

Low depletion may not always be felt to be practical, particularly in low-volume high-throughput screening assays in which there may be a tendency to increase the receptor concentration to maintain the signal from bound ligand while reducing the ligand concentration to minimize cost. However, this involves risks.

An experimental illustration is shown in Figure 3, which shows experimental EC_{50} values for the high-affinity radioligand (–)-[^{3}H]*N*-methylscopolamine ([^{3}H]NMS) binding to M_3 muscarinic receptors plotted against half of the concentration of receptor binding sites added to the assay (Carter *et al.*, 2007). The EC_{50} of [^{3}H]NMS varied by 20-fold, from 10^{-10} to 2×10^{-9} M. A characteristic steepening of the binding curves was observed at high (>90%) radioligand depletion, the Hill slopes rising to 1.8, close to the theoretical limiting value of 2.0, as implied by the non-linear nature of equation 3. As predicted, the EC_{50} values were linearly dependent on the receptor concentration, but the slope factor was 1.3, which is slightly higher than the theoretical value of 1.0. This would be consistent with the presence of a proportion (ca. 25%) of non-bindable radiolabelled impurities in the radioligand preparation, which would cause the systematic overestimation of the EC_{50} value. Testing for non-bindable radioligand is described in section 3.4. The K_d value estimated by extrapolation to zero receptor concentration was 1.07×10^{-10} M (8.2×10^{-11} M if the presence of non-bindable impurities is taken into account).

These data confirm that when $[R_T/2] = K_d$, 50% of the total ligand is bound at half-saturation of the receptor, so that the measured EC_{50} exceeds the K_d by a factor of 2.

- With radioligand depletion, EC_{50} and $[R_T]$ cease to be independent parameters.

Therefore, because $K_d = EC_{50} - [R_T]/2$, the estimation of K_d from the receptor saturation curve, under depletion condi-

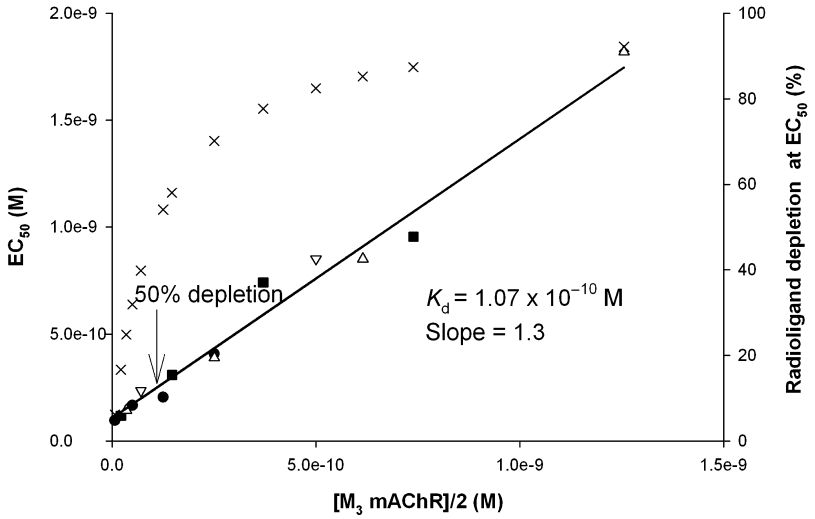

Figure 3 The effect of radioligand depletion on the apparent affinity. EC_{50} values for binding of the high-affinity radioligand [^{3}H]NMS to M_3 mAChRs are plotted against half of the concentration of receptor binding sites added to the assay. The data are taken from Carter *et al.* (2007). Assay volumes ranged from 50 to 1750 μL, and additions of receptor preparation (4 pmol·mg^{-1} protein) from 5 to 50 μg. The straight line shows a linear regression with a slope of 1.3 and *y*-intercept corresponding to $K_d = 1.07 \times 10^{-10}$ M. The crosses show the radioligand depletion at the EC_{50}.

tions, requires accurate determination of the total concentration of receptor sites, as well as the EC_{50}. These measurements must be conducted at high radioligand occupancy and have higher variance than measurements at low occupancy. Furthermore, if non-bindable radiolabelled impurities are present in the radioligand preparation, the EC_{50} may be overestimated. Therefore, the K_d estimate becomes a small difference between two poorly determined larger numbers.

- An accurate value of K_d cannot be determined from a receptor saturation curve if the initial extent of radioligand depletion exceeds 50%.

Binding properties of unlabelled ligands derived from modulation of the receptor-specific binding of the radiolabelled ligand

A central aim of receptor binding studies, particularly from the standpoint of drug screening, is to deduce the binding properties of non-radiolabelled ligands with a specific receptor from their effect on the binding of a radiolabelled reporter ligand.

- In the general case, the unlabelled and radiolabelled ligands bind simultaneously to the receptor to form a ternary complex (Figure 4).

The binding of the first ligand effectively creates a new molecular species. This may change the affinity (and kinetics) of the second ligand, a property referred to as allosteric modulation, and quantified by a cooperativity factor α. Thus, the dissociation constant of the tracer ligand bound to the complex of the receptor with *A* becomes K_{dL}/α. Thermodynamic reversibility demands that the identical cooperativity factor be applied to the binding of *A* to *RL*.

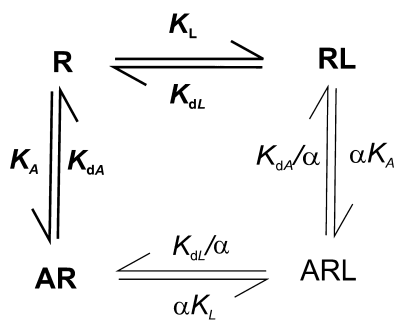

Figure 4 The allosteric ternary complex model of receptor–ligand interactions. Two ligands, *L* and *A*, bind to the receptor separately to give binary complexes RL and AR, governed by dissociation constants K_{dL} and K_{dA} respectively. The simultaneous binding of the two ligands to form a ternary complex, ARL, is subject to a cooperativity factor, α. The thicker arrows delineate a competitive interaction mechanism, when $\alpha = 0$.

- The sign and the magnitude of the cooperativity depend on the nature of both of the interacting ligands, the radiolabelled probe, as well as the unlabelled ligand, a property referred to as probe dependence.

Thus, the measured dissociation constant for the radiolabelled ligand *L* depends on the free concentration of the unlabelled ligand, *A*, in the following way

$$K_{dL,app} = \frac{K_{dL}(1+[A]/K_{dA})}{(1+\alpha[A]/K_{dA})} \quad 5(a)$$

And, symmetrically,

$$K_{dA,app} = \frac{K_{dA}(1+[L]/K_{dL})}{(1+\alpha[L]/K_{dL})} \quad 5(b)$$

Insertion of equation 5(a) into equation 1(b) leads to the following expression for the dependence of net radioligand

binding on the free concentration of the modulating ligand:

$$[RL]+[ARL]=\frac{[L]/K_{dL}\cdot(1+\alpha[A]/K_{dA})}{1+[L]/K_{dL}+[A]/K_{dA}+\alpha[L][A]/K_{dL}\cdot K_{dA}} \quad (5c)$$

When expressed as functions of the free ligand concentrations, the equilibrium binding curves follow simple hyperbolic saturation functions as in equation 1. As the free concentration of one of the ligands (e.g. the modulator) is increased from zero to a receptor-saturating value, so the dissociation constant for the other (the radioligand) changes from an initial value K_d to a final limiting value given by K_d/α.

- Instances of negative allosteric modulators ($\alpha < 1$) are common; examples of positive ($\alpha > 1$) and neutral allosteric modulators ($\alpha = 1$) are also increasingly being discovered (Birdsall and Lazareno, 2005; May *et al.*, 2007).
- For the analysis of experimental data, it is strongly recommended to insert the expression for $K_{dL,app}$ defined by equation 5(a) into equation 3, to yield an expression that is at least compensated for depletion of the radioligand, although not, it should be noted, for depletion of the modulator ligand. This is the course followed below.
- Mutually exclusive competitive ligand binding represents the limiting case of the ternary complex mechanism when $\alpha = 0$.

Classically, this occurs when the binding sites for the ligands overlap, leading to an irresolvable steric clash, so that they cannot bind simultaneously.

- For a competitive interaction, an increase in the concentration of one ligand reduces the affinity of the other without limit, but in the case of negative allosteric modulation, the reduction in affinity reaches a plateau.

Experimentally, the receptor-specific binding of the radioligand becomes zero at a high-enough concentration of an unlabelled competitor, but reaches a non-zero value if the interaction is allosteric. In practise, the difference between competition and negative cooperativity greater than 100-fold ($\alpha < 0.01$) is difficult to detect by means of equilibrium binding experiments alone, and requires investigation of the effect of the allosteric ligand on the kinetics of the radioligand.

For competitive interactions,

$$K_{dLapp} = K_{dL}(1+[A]/K_{dA}) \quad (6)$$

The ratio of K_{dLapp} to K_{dL} is $(1 + [A]/K_{dA})$.

- If a radioligand saturation curve is measured in the presence of a fixed concentration, [*A*], of a competing ligand and compared to one measured in its absence, it will be found to undergo a parallel shift of $\log(1 + [A]/K_{dA})$, when plotted against the log concentration of radioligand.
- Equally, if the binding of a fixed concentration, [*L*], of a radioligand is plotted against log concentration of an unlabelled competing ligand, the resulting inhibition curve will be shifted by a factor $\log (1 + [L]/K_{dL})$.
- These factors, known as the Cheng–Prusoff correction after their popularizers (Cheng and Prusoff, 1973), help to correct the apparent affinity constants for the occupancy of the receptor by the competing ligand.

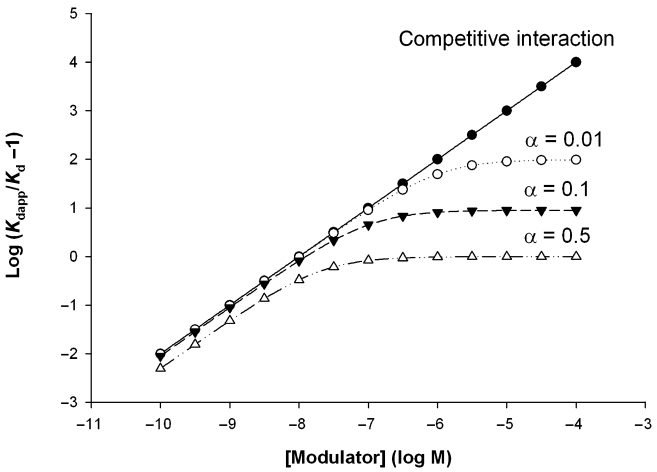

Figure 5 An affinity ratio plot distinguishes a competitive from a negatively cooperative binding interaction. The plot is analogous to a Schild plot of $\log_{10}$(dose ratio – 1) against $\log_{10}$[competitor]. The dose ratio is the ratio of the dissociation constant of the radioligand measured in the presence of the modulator to that in its absence. pK_{dA} is 8.0.

It should be noted that the ligand concentrations used in calculation of the Cheng–Prusoff shift must be the free ligand concentrations corresponding to 50% of the maximum effect, and that these may be influenced by ligand depletion.

- A diagnostic plot for strictly competitive as opposed to allosteric interactions is that of log $(K_{dLapp}/K_{dL} - 1)$ against log[*A*]. Like a Schild plot, this has a slope of 1.0 for a competitive interaction, but progressively deviates from unit slope, eventually reaching a limit governed by the value of α if the interaction is negatively cooperative, as shown in Figure 5.

An early experimental example is shown in Stockton *et al.* (1983). If the interaction is positively cooperative, the binding of the radioligand will be potentiated rather than inhibited by the modulator. These interactions are best quantitated by the fitting of an appropriate model of binding directly to the measured experimental data, as discussed below.

The Cheng–Prusoff shift is well known. However, it is less widely appreciated that:

- The occurrence of radioligand depletion imposes an additional shift on inhibition curves generated by an unlabelled ligand. This is because the free concentration of the radioligand increases as it is displaced from the receptor, opposing the effect of the competing ligand.
- In the case of a simple strictly competitive interaction between two ligands at a single uniform set of binding sites,

a formula for correcting the IC_{50} of the competing ligand to obtain the true K_d was obtained by Goldstein and Barrett (1987).

$$K_{dA} = \frac{IC_{50}}{1 + [L_{50}]/K_{dL} + 2([L_{50}] - [L_0])/[L_0]}$$

The first term in the denominator, $[L_{50}]/K_{dL}$, is recognizable as the Cheng–Prusoff shift. The second is the Goldstein–Barrett depletion correction. If the radioligand depletion is entirely attributable to receptor-specific binding, this can also be written $\delta_0/(1 - \delta_0)$, where $\delta_0 = [RL_0]/[L_T]$ is the ratio of the initial concentration of receptor–radioligand complex to total radioligand. Thus, 50% radioligand depletion causes a twofold Goldstein–Barrett shift even when the Cheng–Prusoff shift is negligible.

- The net shift correction, written in terms of the total radioligand concentration, is

$$1 + [L_T](1 - \delta_0/2)/K_d + \delta_0/(1 - \delta_0) \quad (7)$$

Carter *et al.* (2007) have suggested that, where radioligand depletion cannot be avoided, the IC_{50} values of competing ligands should be measured at a radioligand concentration near to its measured EC_{50} value under the conditions of the assay, and then corrected by a factor equal to $1 + EC_{50}/K_{dL}$ where K_{dL} is the true K_d of the radioligand. They provided experimental data and simulations to support this recommendation. In fact, it can be shown, using equation 7, that the total correction factor applicable to the measured IC_{50} under these conditions is $2 + 0.75[R_T]/K_{dL} = 1.5EC_{50}/K_{dL} + 0.5$, which ranges from 1.0- to 1.5-fold the correction employed by Carter *et al.*, depending on the initial level of radioligand depletion. This accounts for a 1.6-fold discrepancy between the input and calculated values reported in simulations in which radioligand depletion reached 99% (Carter *et al.*, 2007). It should be noted, in addition, that the estimate of the EC_{50} of the radioligand under depletion conditions will be proportionally affected by the presence of non-bindable radiolabelled impurities.

A more serious objection is that if the interaction between the modulating ligand and the radioligand is more complex than competition at a single homogeneous population of binding sites, the presence of radioligand depletion, unlike the Cheng–Prusoff shift, will seriously distort the response curve. For a negative allosteric modulator, apparent affinity will be underestimated, and for a positive modulator overestimated if radioligand depletion is ignored; in both cases, the extent of the cooperativity will be distorted (Avlani *et al.*, 2008). Compensation can be attempted by the use of the exact equation 3, after substitution of equation 5(a). If the interactions are competitive, but represent the sum of two independent populations of binding sites with different affinities for the competing ligand, radioligand displaced from the high-affinity population will rebind to the low-affinity population as the concentration of competitor increases. In an extreme case, the presence of a high affinity subpopulation may be completely obscured (Wells *et al.*, 1980). Exact equations for analysis of the two-site case exist,

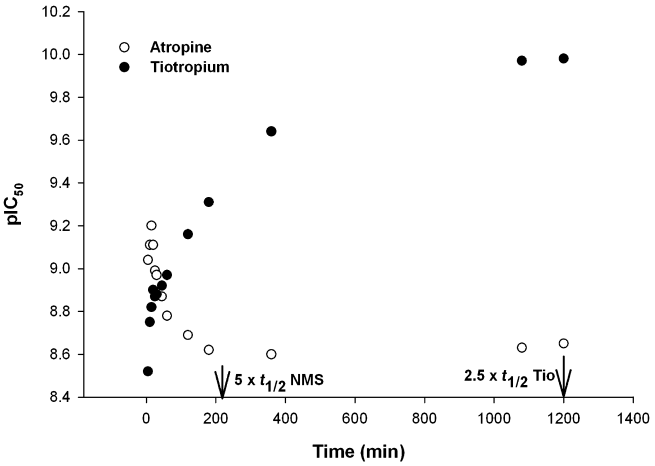

Figure 6 Opposite time dependences of the apparent inhibition constants of a 'fast' and a 'slow' competitor. *p*IC_{50} values for atropine (a fast competitor) and tiotropium (a slow competitor) were determined at room temperature by competition with [^{3}H]NMS (3.5×10^{-10} M) for binding to M_3 mAChRs expressed in CHO cells. Incubation times ranged from 5 to 1200 min. The data are replotted from Dowling and Charlton (2006).

but are algebraically complex (Wang and Jiang, 1996; Hulme, 1999) and difficult to use for quantitative data analysis. It must be concluded that:

- In ligand modulation experiments, as well as in saturation studies, radioligand depletion over 50% strongly increases parameter correlation, increases error and should be avoided if at all possible.

The forgoing analysis has all been subject to the assumption that the binding assays have achieved equilibrium, $[RL]/[RL_{eq}] > 0.97$. However:

- The presence of a competing unlabelled ligand will lengthen the equilibration time of the radiotracer.

Even if the competitor binds rapidly compared to the tracer ($k_{off,A} > 10 \times k_{off,L}$), a high concentration still reduces the effective tracer on rate, so that the equilibration time becomes limited by the tracer k_{off} irrespective of the time-course in the absence of the competitor, which may be fast if the initial tracer ligand occupancy is high.

- When the rate constants of the competing ligand are slower than those of the tracer ligand, it is the k_{off} of the competing ligand that determines the rate of approach to equilibrium.

In this case, a biphasic approach to equilibrium will be seen, which may include a marked overshoot of tracer ligand binding. Dowling and Charlton (2006) studied the binding of a 'fast' antagonist, atropine (k_{off} = 0.27 min^{-1}), and a 'slow' antagonist tiotropium (k_{off} = 0.0015 min^{-1}) to M_3 mAChRs by competition with a concentration of [^{3}H]NMS sufficient to give ca. 90% receptor occupancy (Figure 6). The apparent potency of atropine decreased with time, achieving its final value after ca 220 min, corresponding to $5 \times t_{1/2}$ for dissocia-

tion of the tracer [^{3}H]NMS; in contrast, tiotropium may not have achieved full equilibrium even after 1200 min, which represents only 2.5 × $t_{1/2}$ for dissociation of the competitor. Given sufficiently precise data, the analysis of such time courses provides estimates of the kinetic rate constants of the unlabelled competing ligands (Motulsky and Mahan, 1984; Dowling and Charlton 2006).

- The effects of allosteric ligands on tracer kinetics may be even more profound.

This is because in the limit the tracer binds to, or dissociates from, the complex of the receptor with the second ligand, yielding a parameter designated $k_{offL,occ}$. Acceleration and deceleration of the tracer kinetics are both possible. Often, the slowing will be extreme; the allosteric ligand may 'plug' access to the binding site so that the tracer can neither enter nor leave without prior dissociation of the allosteric partner. In fact:

- The simplest test for allosterism is to vary the concentration of the putative cooperative ligand, and measure its effect on the dissociation rate constant of the tracer.

At one extreme, if the allosteric ligand dissociates much more rapidly than the tracer ligand so that it remains in equilibrium throughout the dissociation process, the apparent dissociation rate constant changes monotonically from k_{offL} to $k_{offL,occ}$, and analysis of the resulting curve yields an estimate of K_{dA}/α, which is the dissociation constant of the allosteric ligand bound to the receptor–tracer complex. At the other extreme, if the allosteric ligand dissociates much more slowly than the tracer, the occupied and unoccupied receptors behave as independent populations, and the observed time-course will be the sum of the separate exponentials describing dissociation from the two populations (Lazareno and Birdsall, 1995).

For the association reaction in the presence of a receptor-saturating concentration of a rapidly dissociating allosteric ligand, $k_{on,appL} = k_{offL,occ}(1 + \alpha.[L]/K_{dL})$ so that the apparent association rate of a low concentration of the tracer ligand is dominated by its dissociation rate from the ternary complex, which may become vanishingly small.

- Allosteric interactions can produce a 'kinetic artefact', whereby the allosteric ligand inhibits the binding of the tracer ligand by slowing its association rate to zero, even though its effect on the equilibrium binding of the tracer ligand is neutral or positively cooperative (Lazareno and Birdsall, 1995).
- This could be confused with apparent competitive inhibition in the context of screening assays.

The upshot is that it is vital to remember that:

- The time-course of tracer binding, measured alone, is not a good guide to the time-course in the presence of a second unlabelled ligand.

In general, the rate of approach to equilibrium is dominated by the kinetics of the slowest reaction step. A simple rule is that the binding reaction should be incubated for five times the half-time of the slowest step in the reaction mechanism if equilibrium is to be achieved.

- A simple assay methodology to address this issue is therefore to assess how IC_{50} varies with incubation time.

If IC_{50} is constant with two sufficiently different incubation times, the assay is at equilibrium for the compound under study. If, however, the compound becomes more potent with incubation time, then this implies non-equilibrium conditions and thus questionable data (Heise *et al.*, 2007).

The practicalities of radioligand binding assays

In the following sections, we outline some important considerations in the practical implementation of equilibrium binding assays.

Choice of radioligand

The availability of radioligands for binding studies is constrained by the pharmacology of the receptor and the suitability of its ligands for radiolabelling. For [^{3}H]ligands, typical specific radioactivities are in the range of 50–100 Ci·mmol^{-1} (two to four tritium atoms per molecule). [^{125}I] ligands often have an initial specific activity of 2190 Ci·mmol^{-1}. Radioligand stocks are usually provided at 1 mCi·mL^{-1}, with a concentration of 1–2 × 10^{-5} M for [^{3}H]ligands.

The choice of radioligand may depend on the aim of the experiment. Determination of B_{Max} and K_d requires measurements ranging over occupancies of 10–90%. For a radioligand with a K_d of 10^{-9} M, 90% occupancy implies a (free) radioligand concentration of 10^{-8} M, representing up to 1 μCi (37 kBq) of [^{3}H] per assay. This probably represents the practical upper limit of radiotracer usage, unless the radioligand is first diluted with unlabelled ligand to reduce its specific radioactivity: in this case, the unlabelled ligand should be chemically identical to the labelled ligand, and the receptor-specific binding will be reduced in proportion. The maximum usable concentrations of ligands labelled with other radioisotopes, such as [^{125}I], may be substantially lower.

- Radioligands with K_d < 10^{-9} M should be used for measurements of B_{Max} and K_d.
- Specific radioactivities less than 5 Ci·mmol^{-1} are unlikely to be useful.

Binding equilibrium must be reached. The half-time for radioligand dissociation should be measured, and an incubation time exceeding 5 × $t_{1/2}$ must be used. It is necessary to check that the receptor preparation is stable over the necessary time period.

- Proteolysis may be occurring if specific binding peaks, and then diminishes over time, particularly if the instability is greater at higher concentrations of the membrane fraction.

- Proteolytic inhibitors appropriate to the receptor preparation should be added, if needed, but they should be examined for direct effects on binding.

The polarity of the ligand may affect B_{Max} and K_d. A study on mAChRs expressed in the neuroblastoma cell line SK-N-SH illustrates this point (Fisher, 1988). At low temperature, the B_{Max} value for the hydrophilic antagonist [^{3}H]NMS was significantly lower than that of the more lipophilic antagonist [^{3}H]QNB, whereas at 37°C the values were similar. This study suggested that in these cells, there were at least two pools of receptor that were differentially labelled by the liphophilic versus the hydrophilic antagonist at low temperatures, but this was not evident at 37°C.

Alternatively, a frequent aim is to estimate corrected IC_{50} or pK_d values for a series of ligands from inhibition of the binding of the radiolabelled tracer ligand by a series of serial dilutions of the unlabelled ligands. A useful empirical rule is that if the assay is directed towards screening for inverse agonist molecules, then the radioligand used should itself be an inverse agonist at the receptor as the structure–activity relations of the high-affinity agonist binding, G protein-coupled, state of the receptor are often different from those of the uncoupled state, which favours inverse agonists (Sharif *et al.*, 1995).

- 'Setting Up Screening Assays for Modulators of Radioligand Binding' contains guidelines for setting up inhibition assays to obtain a usable level of signal while avoiding depletion artefacts.

Optimizing the recovery of bound ligand in filtration assays

Receptor–radioligand complexes are separated from free ligands by sucking the incubation medium through filters (such as glass fibre) to trap the cell membranes. The filters are then washed several times with buffer to remove residual unbound ligand and any ligand that can be rapidly washed from non-specific binding sites. Ideally, the receptor–ligand complex will not dissociate significantly during washing, and will be completely trapped by the filters. If the wash time is a typical 10 s, less than 10% dissociation requires a k_{off} < 0.01 s^{-1}. If we assume k_{on} values of 10^6–10^7 $M^{-1}s^{-1}$, which are typical at room temperature (c.f. Figure 2B), the corresponding K_d values are 10^{-8}–10^{-9} M.

- Filtration is not suitable for radioligands with $K_d > 10^{-8}$ M, if the washes are conducted at room temperature.
- The use of ice-cold wash buffer is the default recommendation. It can extend the usable range by up to 100-fold (K_d = 10^{-7}–10^{-6} M); k_{off} is often greatly reduced at low temperature.

It may also be possible to add a neutrally cooperative allosteric modulator to the wash buffer that strongly reduces the dissociation rate constant (see 'Binding Properties of Unlabelled Ligands Derived from Modulation of the Receptor-specific Binding of the Radiolabelled Ligand'). It is advisable to perform a systematic study of recovery of total and non-specific binding as a function of number of washes.

It is important to choose the correct filters for the job. Thicker GFB filters will give more complete recovery of small membrane fragments than the thinner GFA filters, but may extend the wash time. Pretreatment of the filters may be performed. For instance, soaking with 0.05–0.125% polyethylene imine for 10 min gives them a positive surface charge that may help to trap negatively charged membrane fragments. This also minimizes non-specific binding of cationic (but not anionic!) ligands. Again, a systematic comparison is desirable.

Measuring non-specific binding

The measured signal from binding assays is the sum of the receptor-specific element and non-specific binding to components of the assay system. The latter arises partly from the entrapment of radioligand in the filters used for performing the separation, and partly from low-affinity binding to membrane proteins or partitioning into phospholipids. These low-affinity processes are usually non-saturable at the ligand concentrations used in receptor binding studies, and are modelled by the product of a coefficient of non-specific binding, N, and the free radioligand concentration; when the concentration of the membrane preparation is varied, N can be expanded to include both components; $N = N_S + N_R.[R_T]$. Typical values for N_S are in the range 10^{-4}–10^{-3}, and for N_R 10^{-4}–10^{-3} nM^{-1} for cationic ligands binding to muscarinic receptor preparations, for example.

Non-specific binding adds an extra term to the conservation equation for the radioligand, which becomes $[L] + N[L] + [RL] = [L_T]$. Equation 3 for the concentration of receptor–ligand complex is also slightly modified:

$$[RL] = \frac{([R_T] + [L_T] + K'_d) - \sqrt{([R_T] + [L_T] + K'_d)\,\hat{}\,2 - 4[R_T][L_T]}}{2} \quad (3b)$$

where $K'_d = (1 + N)K_d$

$[L]$ is calculated as $([LT] - [RL])/(1 + N)$, and the total measured ligand binding is given by the sum of the receptor-specific and non-specific components:

$$[L_{Bound}] = [RL] + N([LT] - [RL])/(1 + N) \quad (3c)$$

This is numerically equivalent to an expression developed by Swillens (1995).

- Equations 3b and 3c should always be used to analyse radioligand saturation curves in the presence of non-specific binding.

The accurate estimation of N is necessary for the analysis of both radioligand saturation and inhibition data. This is critical to distinguish competitive from negatively cooperative inhibition of tracer ligand binding, which may only be diagnosed by residual specific binding of the radiotracer persisting at high concentrations of the unlabelled ligand.

Ideally, non-specific binding should be estimated by incubating the receptor preparation with concentrations of the radioligand spanning the entire range to be used together with a sufficient concentration of an unlabelled, strictly competitive ligand, I, having a sufficient affinity to maintain at

least 99.9% occupancy of the receptor at the highest radioligand concentration used, L_{Max}.

- For the determination of non-specific binding, the concentration of the competing ligand [*I*] must be >1000.K_{dI}(1 + [L_{Max}]/K_{dL}). For instance, if the radioligand is used at 10 × K_{dL}, then the non-radiolabelled competitor will need to be used at 10 000 × K_{dI}.
- It may be misleading to define receptor-specific binding as the component of radioligand binding inhibited by a large excess of the corresponding unlabelled ligand.

This will also inhibit radioligand binding to non-receptor sites which, although of low affinity, may have high binding capacity. Instead, it is desirable to use an unlabelled ligand that is chemically distinct from the radiotracer, while maintaining high affinity.

A possible hazard is that a tracer ligand that can exist in a non-ionized form may access a membrane compartment that is inaccessible to a polar ligand employed to define non-specific binding. An example of this is shown in Figure 7, in which inhibition of the binding of the high-affinity tertiary amine antagonist (–)-[^{3}H]-3-quinuclidinyl benzilate ([^{3}H]QNB) to M_1 mAChRs was inhibited by two competing ligands, (–)-*N*-methylscopolamine (NMS), which is a quaternary amine, and (–)-scopolamine, the tertiary analogue of NMS. Unlike QNB and scopolamine, NMS cannot easily cross a lipid bilayer to penetrate sealed vesicles, reminiscent of the B_{Max} differences described in 'Choice of Radioligand'. The presence of a minor population of less accessible sites in the membrane preparation was suggested by the failure of a single-site model of binding to fit the NMS-[^{3}H]QNB competition curve at the higher concentrations of competing ligand used. The inclusion of 10% of binding sites with a lower apparent affinity resolved this anomaly. In contrast, the scopolamine-[^{3}H]QNB data were fitted by a single site model. In this case, scopolamine (10^{-5} M) rather than NMS should be used to define the non-specific binding of [^{3}H]QNB.

- Ideally, several different unlabelled competitors should all yield statistically indistinguishable estimates of non-specific binding.

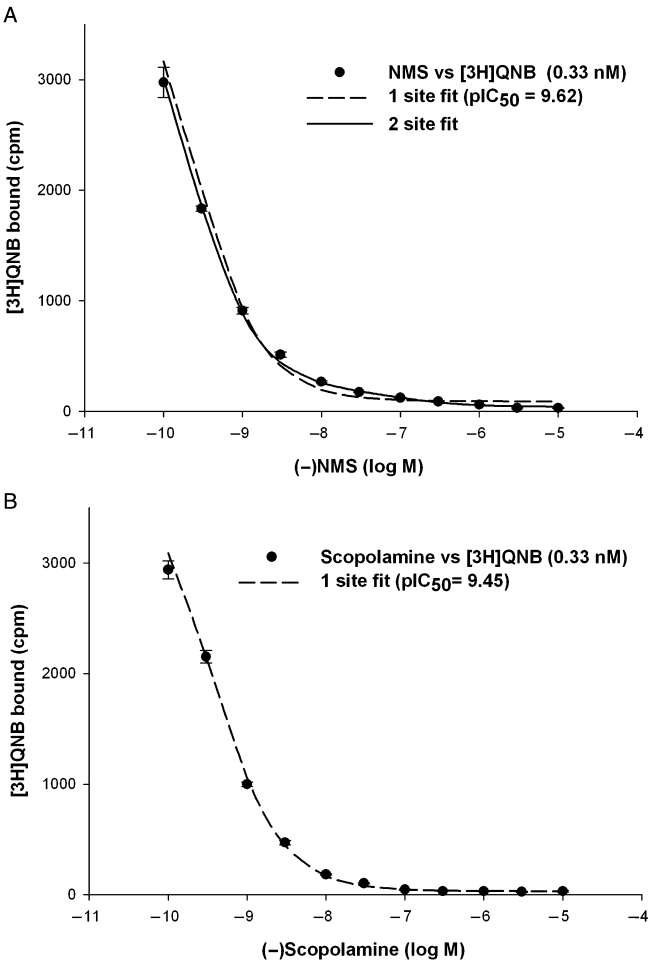

Figure 7 Choice of unlabelled ligand to define non-specific binding for a lipophilic radioligand. Binding of (–)[^{3}H]quinuclidinyl benzilate (3×10^{-10} M), a tertiary amine muscarinic antagonist, was measured over 24 h using a recombinant M_1 muscarinic receptor construct (50 fmol·mL^{-1}) expressed in *Escherichia coli* spheroplast membranes suspended in 50 mM sodium phosphate, pH 8.0: (A) Inhibition of [^{3}H]QNB binding by a quaternary amine antagonist, (–)*N*-methylscopolamine, could not be fitted by a single-site inhibition curve, but required the addition of about 10% of sites with ca. 50-fold lower affinity; (B) inhibition of [^{3}H]QNB binding by scopolamine, the tertiary analogue of NMS, was adequately described by a single site model for a homogeneous set of binding sites.

Quality control checks on the radioligand: bindability and specific radioactivity

For a commercially available ligand, the manufacturer's data sheet will give information about the specific radioactivity of the ligand on a reference date, the radioactive content of the preparation, its chemical purity and advice on its storage and handling. One simple piece of advice is always to allow vials of radioactive ligands, which are often in ethanolic solution stored at –20°C, to equilibrate to room temperature before opening them, to prevent the condensation of water vapour. In the case of custom-synthesized or laboratory-labelled radioligands, handling and purity data may be less well established. The default assumptions are that the stated specific activity of the radioligand is correct, and that the material is chemically pure and 100% competent for receptor binding. However, this may not be the case.

- It is highly desirable to check the bindability and specific activity of the radioligand before embarking on a major series of assays.

Non-radioactive tight-binding impurities, for instance, left over from the starting material, may be a hazard. If undetected, the presence of such contamination will lead to overestimation of the apparent affinity constant of the radioligand, and underestimation of the apparent concentration of receptor binding sites. It may also artefactually limit the association rate constant (Lazareno and Birdsall, 2000). This can have real consequences (Sum *et al.*, 2001).

The opposite situation arises when the radioligand is contaminated with non-bindable radiolabelled impurities. These may accumulate. For instance, the active enantiomer of a radioligand may racemize to the inactive form during storage.

- If undetected, the presence of non-bindable radiolabelled impurities will cause the overestimation of the apparent free radioligand concentration, particularly under tracer depletion conditions. This will lead to underestimation of its affinity.

Because of the symmetry of equation 3, depletion due to receptor binding can be exploited to estimate the bindable fraction of the radioligand, by carrying out measurements at different concentrations of the receptor preparation. If concentrations such that $[R_T] > 3 \times K_d$ are achievable, then a good estimate of radioligand bindability can be obtained. The set of data in Figure 8A shows the binding of [^{3}H]NMS to M_1 mAChRs at a series of dilutions of the receptor preparation that yielded binding site concentrations of up to 0.5 nM, ($5 \times K_d$). Apparent radioligand depletion at the lowest [^{3}H]NMS concentration used was up to 73%.

The binding curves were analysed using equations 3b and 3c for depletion-compensated radioligand binding, modified to use receptor dilution as an independent variable.

- The true concentration of bindable radioligand (nM) is calculated using the expression $[L_{TB}] = FrB^*(LT\text{dpm} - Bgd)/(2220^*SPact^*V)$ where *LT*dpm is the measured total radioligand added to the assay (dpm), *Bgd* is the counter background, *SPact* is the radioligand-specific activity, *V* is the volume of the assay and *FrB* is the fraction of bindable radioligand.

FrB was one parameter determined by least-square fitting. In addition, the expanded definition of the coefficient of non-specific binding $N = N_S + N_R.[RT]$ allowed it to vary at different concentrations of the membrane fraction. The equations provided an excellent global fit to the data set. The bindability of the [^{3}H]NMS preparation was estimated to be 0.745 ± 0.038, significantly less than the assumed value of 1.0 ($P < 10^{-5}$ using an *F*-test to compare fits obtained with *FrB* restricted to 1.0, or allowed to vary; see legend to Figure 8A), and similar to the estimate needed to describe the data in Figure 3 ('The Effect of Radioligand Depletion on Tracer Association and Equilibrium Binding'). N_S and N_R were both ca. 5×10^{-4}.The very low non-specific values reflect the favourable properties of the quaternary ammonium ligand [^{3}H]NMS in the filtration binding assay; when using non-polar ligands, values 10× this are common.

- Both bindable and non-bindable ligand contribute to non-specific binding.

A simplified method for analyzing radioligand bindability is to plot 1/dpm bound against $1/[R_T]$, extrapolating the plot to infinite receptor concentration. Applied to the lowest [^{3}H]NMS concentration, this gave the straight line shown in Figure 8B, yielding an apparent bindability of 83%. However, this is an overestimate because it does not allow for diminished non-specific binding of the radioligand caused by radioligand depletion at the highest receptor concentrations used (Schumacher and Von 1994).

- Specific radoactivity is a second parameter needed to calculate the true concentration of radioligand added from the input radioactivity.

Assuming that the binding affinities of the radiolabelled and unlabelled ligands are identical:

- The specific radioactivity of the radiolabelled ligand can be estimated by systematically comparing the pK_d value obtained by a tracer ligand saturation experiment with the value from a homologous competition experiment in which the unlabelled ligand is used to inhibit the binding of the labelled ligand.

It should be noted that the requirement of equal affinity requires that the unlabelled and labelled ligands be chemically identical. Thus, if the ligand is labelled with [^{125}I], the unlabelled ligand must be the iodinated form of the unlabelled ligand rather than the non-iodinated form, which is not guaranteed to have the same affinity.

An example, for [^{3}H]NMS, is shown in Figure 9. The direct saturation (Figure 9A) and homologous competition (Figure 9B) experiments were analysed simultaneously as a single data set using equation 3b, with the concentration of unlabelled ligand added as a separate independent variable. The estimated specific activity of the radioligand was 67.4 ± 2.7 Ci·mmol^{-1}, acceptably close to the manufacturer's value of 75 Ci·mmol^{-1} given the uncertainties of the measurements.

A secondary check on the consistency of radioligand binding assays is to use a second radioligand to perform saturation assays on the same population of receptor binding sites. If the specific activities of both ligands are accurate, the estimated total concentrations of binding sites should not be significantly different. If they are, then either one (or both) of the specific activities is incorrect, or there is a subpopulation of binding sites that cannot be accessed by one of the ligands.

Setting up screening assays for modulators of radioligand binding

In a screening assay, a key constraint is provided by the desired level of signal from the receptor–radioligand complex in the assay in the absence of any additional ligands.

- Thus, 1500 cpm provides a 95% confidence limit of 5% after counting for 1 min, while 300 cpm gives the same confidence level after 5 min. For a counter with an efficiency of 50%, these counts correspond to concentrations of ca. 30 and 5.5 fmol of receptor ligand complex in a 1 mL assay for a radioligand with a specific activity of 50 Ci·mmol^{-1}.

We have seen that ligand depletion seriously distorts both saturation and inhibition binding data. As a general rule, depletion should be held to less than 10%. Levels of 10–30% may allow parameter estimates to be obtained, although their reliability may be somewhat compromised. Levels exceeding 50% may invalidate the experiment.

- Let σ denote the concentration of receptor–ligand complex that gives the desired level of signal. For instance, this

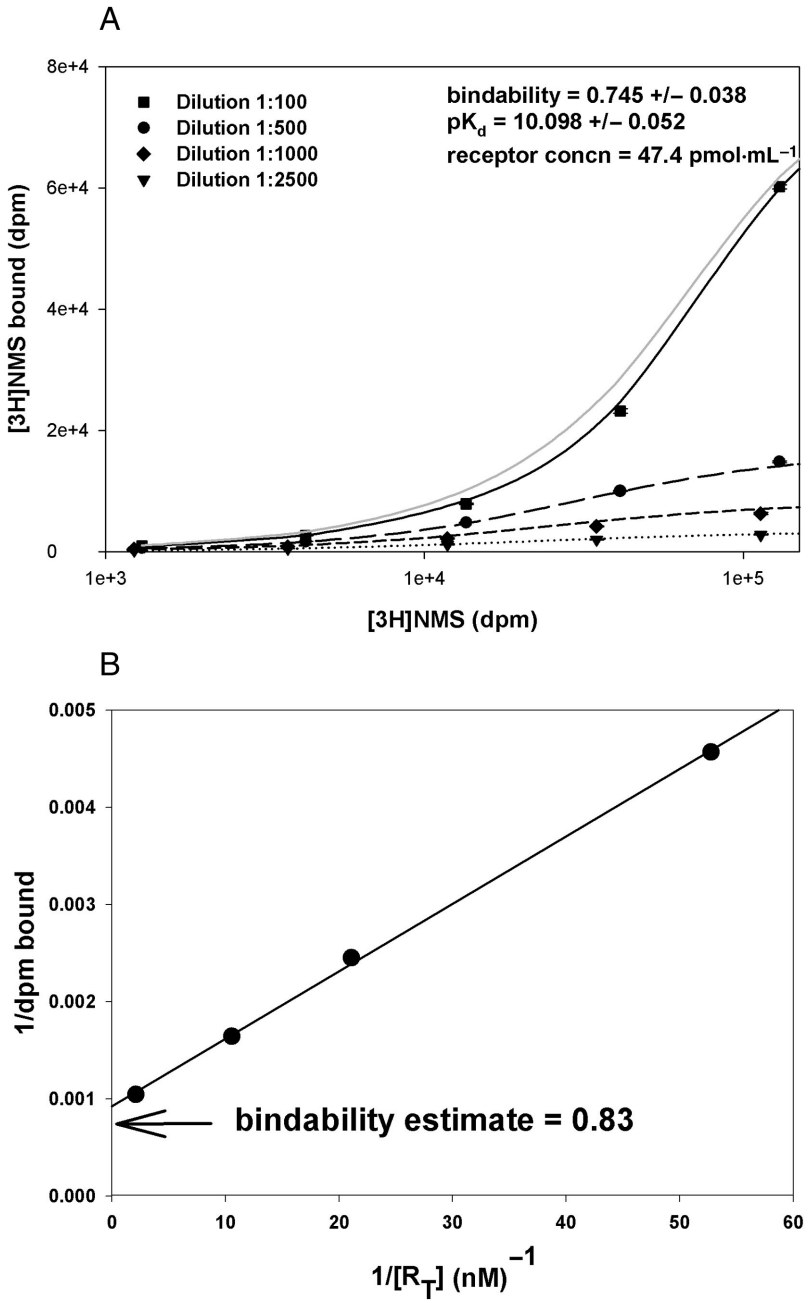

Figure 8 Quality control checks on the radioligand: bindability. The equilibrium binding of (–)[^{3}H]NMS to recombinant M_1 mAChRs was measured after 60 min at 30°C in 50 mM sodium phosphate, pH 8.0. Assay volume was 1.0 mL. (A) Determination of the fractional bindability, *FrB*, of a batch of [^{3}H]NMS. Saturation binding assays (0.0078–2.4 nM [^{3}H]NMS).were performed using a range of dilutions of an M_1 mAChR preparation initially containing 47.4 pmol·mL^{-1} binding sites (13 pmol·mg^{-1} protein). Non-specific binding was measured using atropine (10 μM). The data were globally fitted to equations 3b and 3c with the total ligand concentration calculated as [L_{TB}] = *FrB**(*LT*dpm – *Bgd*)/(2220**SPact***V*). The full lines show the set of fitted curves. *FrB* was estimated to be 0.75 ± 0.05. Restriction of *FrB* to 1.0 gave a poor fit to the data at the highest mAChR concentration (grey line). An *F*-test on the sum of squares of the weighted residuals gave $P < 10^{-5}$ with respect to the unrestricted fit. pK_d was 10.10 ± 0.05. The coefficients of non-specific binding were: N_S, 3.7×10^{-4}; N_R, 5.2×10^{-4} nM^{-1}. (B) Plot of 1/dpm bound versus 1/[R_T] for the lowest concentration of [^{3}H]NMS. Comparison of the *y*-intercept with the inverse of *LT*dpm, the total radioactivity added to the assay (arrow), gave an estimated *FrB* of 0.83.

might be 30 fmol·mL^{-1} in a 1 mL assay, or 150 fmol·mL^{-1} in a 0.2 mL assay. Let the target level of depletion be δ_0 (preferably ≤0.1). Then, the total concentration of radioligand (assumed to be 100% bindable) is $[L_T] = \sigma/\delta_0$. What concentration of receptor binding sites should be used?

- From the definition of the equilibrium constant and the receptor conservation equation

$$[R_T] = [RL] + \frac{K_d[RL]}{([L_T] - [RL])} = \sigma + \frac{K_d\delta_0}{(1-\delta_0)} \quad (8)$$

For the above example of a signal of 1500 cpm from 1 mL assay volume, σ is 0.03 nM, $[L_T]$ is 0.3 nM and $[R_T]$ is 0.14 nM (140 fmol/assay), for a radioligand with a pK_d of 9.0 to yield a

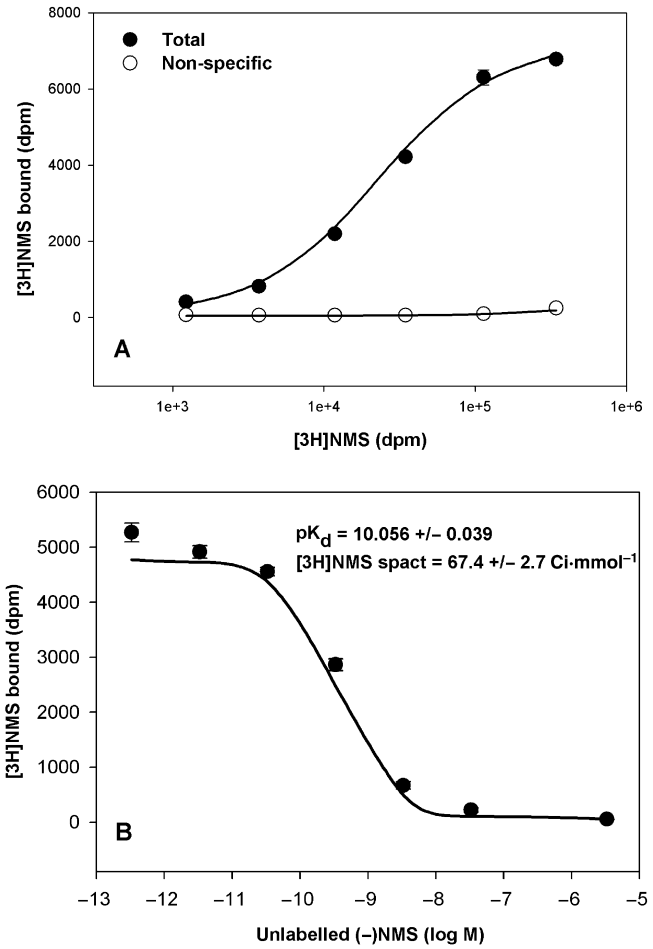

Figure 9 Quality control checks on the radioligand: specific radioactivity. Estimation of the specific radioactivity of a batch of [^{3}H]NMS. Assay conditions were as in Figure 8. A direct saturation curve (A) was compared to a homologous competition curve (B) using a receptor concentration of 50 fmol·mL^{-1}. The full data set from (A) and (B) was analysed simultaneously, with *FrB* fixed at 0.745, giving an estimated specific radioactivity (*SPact*) of 67.4 ± 2.7 Ci·mmol^{-1}. The pK_d of NMS was 10.06 ± 0.04.

depletion level of 10%. The radioligand depletion can be further decreased either by increasing $[L_T]$ or decreasing $[R_T]$ by increasing the assay volume while maintaining $[L_T]$. Decreasing the assay volume requires a compensating increase in radioligand concentration to maintain the same level of depletion. There is a trade-off between the extent of radioligand depletion, the specific : non-specific binding ratio and the shift correction. The shift correction is calculated by substituting $[L_T]$ and δ_0 into equation 7. For a 1 mL assay, it is modest for this example, 0.14 log units, but would rise to 1.47 log units for a radioligand with a pK_d of 11 for the same level of signal. The corresponding values for a 0.2 mL assay are 0.40 and 2.16 log units.

- An initial signal corresponding to about 10 fmol·mL^{-1} of receptor ligand complex sets a natural upper bound on the affinity of [^{3}H] ligands that can be used in competition binding assays. This cannot exceed ca. 10^{11} M^{-1} if K_d is to remain above $[R_T]$, so that radioligand depletion remains below 50%.

Higher working affinities may be possible for [^{125}I] ligands, which have a higher specific activity, permitting the detection of a smaller absolute amount of receptor–ligand complex.

- For very high-affinity ligands, the limiting factor may be the time taken to achieve equilibrium.

For example, at room temperature, the muscarinic antagonist QNB (K_d = 30 pM) has a k_{off} of 0.003 min^{-1}, while NMS has a similar affinity but has a k_{off} of 0.017 min^{-1}. Thus, at their respective K_d values, QNB will take approximately 10 h to reach equilibrium, but NMS less than 2 h. Evidently, longer incubations make greater demands on the stability of the receptor preparation.

- Non-specific binding sets a lower bound on the working radioligand affinity.

Non-specific binding under the assay conditions may be calculated from the expression $[NS] = [L_T]N/(1 + N)$ where $N = N_S + N_R[R_T]$ is the sum of the system-dependent and receptor preparation-dependent components (c.f. Figure 8A legend). For a value of the receptor-dependent non-specific binding coefficient of N_R = 0.001 nM^{-1}, a pK_d of 6 gives approximately equal specific and non-specific binding when the receptor-specific signal is 30 fmol·mL^{-1}. This is of the same order as the off-rate-determined limit. Again, the kinetic factors determining the loss of specifically bound radiolabelled ligand during the filtration process may become the more important limitation.

The values of $[R_T]$ and the Cheng–Prusoff shift together determine the effective range of affinities for unlabelled competing ligands that can be studied in a particular assay.

- The pIC_{50} values of competing ligands may be estimated by fitting the Hill equation to the inhibition curves: $\text{dpm} = \{\text{Top} - \text{Bottom}\}/[1 + 10^{nH*(pIC_{50}+\log A)}] + \text{Bottom}$. The curves range from a 'top' value to a 'bottom' value, which for competitive (but not allosteric) ligands should correspond to non-specific binding; logA is $\log_{10}$ of the competing ligand concentration. The primary parameters characterizing the ligand interaction are the pIC_{50} and the slope factor, *nH*. In any set of assays, sufficient replicates (four or more) must be used to allow the mean and SEM of the total ('top') and non-specific ('bottom') binding (using the standard ligand) to be determined accurately.

In the absence of competing interactions, the measured IC_{50} of the unlabelled ligand, like the EC_{50} of the radioligand, cannot fall below the 'assay limit' of $[R_T]/2$. However, by raising the concentration of radiotracer, a high-affinity competitor can be 'forced' to a lower apparent affinity, bringing the competition curve into range.

- The effective assay limit is given by $K_{dA} > [R_T]/(1 + [L_T](1 - \delta_0/2)/K_{dL})$. Competition from the radioligand enhances the working range of the assay by the factor $(1 + [L_T](1 - \delta_0/2)/K_{dL})$. This may be a substantial factor for a high-affinity radiotracer. It is still necessary to ensure that the assays achieve equilibrium.

Of course, the use of a higher tracer concentration will also diminish its specific : non-specific binding ratio. It should be noted that an allosteric inhibitor will show reduced maximal inhibition of the tracer ligand binding when subjected to this manoeuvre.

Determining the mechanism of ligand interactions at equilibrium
The outcome of a screening campaign is (hopefully) a number of 'hits' that fulfil preset requirements of ligand potency. The question then arises:

- What is the mechanism of interaction of a particular ligand with the receptor in relation to the radiotracer ligand, which usually binds to the orthosteric site?

Hints may emerge from the screening experiments. For instance, if binding of the radioligand is potentiated, or is inhibited but plateaus at a value significantly greater than the true non-specific binding, then the mechanism of interaction must be allosteric. However, the reverse is not true. If the ligand completely inhibits binding of the radiotracer, it may still not be interacting competitively; an allosteric mechanism, such as neutrally cooperative binding accompanied by an extreme form of the kinetic slowing artefact pointed out in 'Binding Properties of Unlabelled Ligands Derived from Modulation of the Receptor-specific Binding of the Radiolabelled Ligand' cannot be excluded.

- A logical and powerful extension of an initial binding screen helps to answer this question: simultaneous equilibrium binding assays using a wide range of radioligand concentrations.

This multi-ligand design (Rovati, 1998) can differentiate strictly competitive from negatively cooperative mechanisms of interaction, which only become evident at high levels of radioligand occupancy.

- A revealing experimental format is to use three different radioligand concentrations, such as 0.2×, 2× and 10× the radioligand K_d. The entire data set is subjected to global analysis using the allosteric ternary complex model corrected for radioligand depletion.

An empirical slope factor is added to equation 5 before substitution into equation 3b (e.g. $[A]/K_{dA}$ is replaced by $([A]/K_{dA})^{nH}$. This allows the inhibition curves to deviate from simple hyperbolic behaviour. Such an experiment yields, simultaneously: (i) an estimate of pK_{dL} for the tracer ligand; (ii) an estimate of pK_{dA} for the unlabelled inhibitor; (iii) the slope factor of the inhibition curve; (iv) an estimate of the cooperativity, α, between the labelled and unlabelled ligands; (v) the concentration of binding sites; and (vi) the coefficient of non-specific binding.

An experimental example is shown in Figure 10. This shows inhibition of the binding of [^{3}H]NMS to the M_1 mAChR by a selective agonist, 77-LH-28-1 (Lebon *et al.*, 2009).

In the case of the wild-type receptor, a strictly competitive model of binding provided an excellent fit to the data;

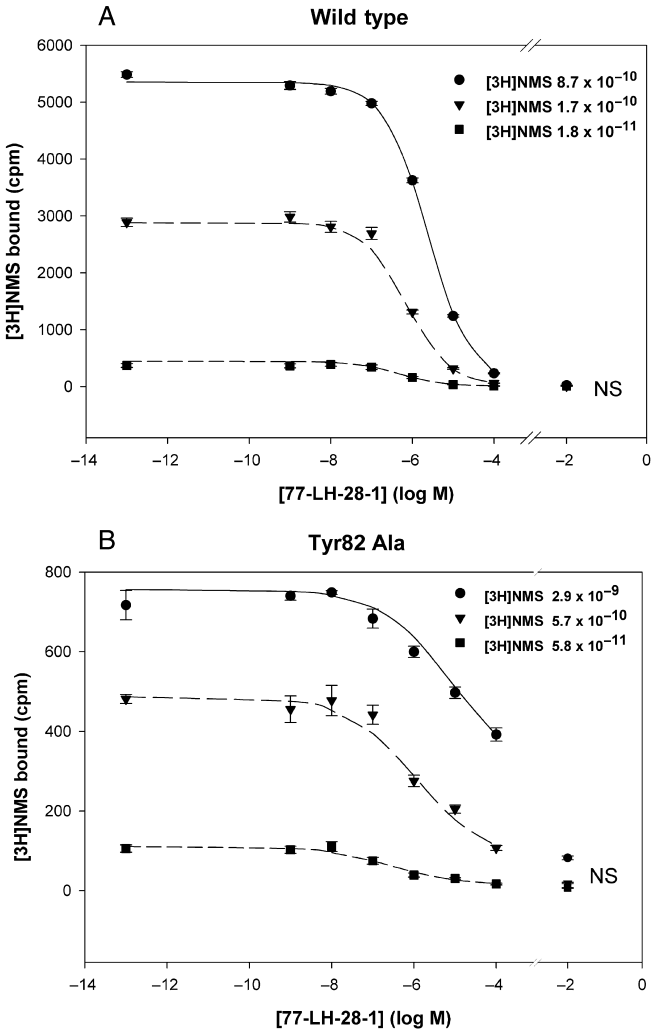

Figure 10 Probing the mechanism of interaction between a test ligand and the radiotracer using several concentrations of radioligand. Binding of [^{3}H]NMS to wild-type and mutant M_1 mAChRs expressed in membranes from COS-7 cells was measured at 30°C for 2 h in 20 mM Na HEPES, 100 mM NaCl, 1 mM $MgCl_2$, pH 7.5. Concentrations of [^{3}H]NMS equivalent to 0.2×, 2× and 10× K_d were used. Serial dilutions of the agonist 77-LH-28-1 in dimethyl sulphoxide were added to the assays (final DMSO concentration 1%). Non-specific binding was measured with 10^{-5} M scopolamine. Assays were performed in quadruplicate. Maximum radioligand depletion was 10%. Data were globally fitted to the allosteric ternary complex model equation 5a embedded in equation 3b, and modified to allow non-unitary slopes for the competition curves. (A) Wild-type receptor showing competitive inhibition; pK_{dL} ([^{3}H]NMS), 9.74; pK_{dA} (77-LH-28-1), 6.54; *nH* 0.84; log(α) was fixed at –6. (B) Tyr82 Ala mutant showing allosteric inhibition: pK_{dL} 9.45; pK_{dA} 6.67; *nH* 0.50; log(α), –1.33.

[^{3}H]NMS binding was reduced to the non-specific level by a sufficient concentration of 77-LH-28-1. However, for the Tyr82 Ala mutant, the selective agonist failed to give complete inhibition of [^{3}H]NMS binding at the higher levels of radioligand occupancy, even though the radioligand had a reduced affinity for the mutant receptor. To account for this, the value of α was 0.046, significantly greater than zero. This behaviour might have been missed if only one low concentration of [^{3}H]NMS had been used. It should be noted that because α and K_{dA} occur as a ratio in the denominator of equation 5a,

they are highly correlated during the performance of the fit (Avlani *et al.*, 2008), somewhat increasing the interdependence and standard errors of the two parameter estimates.

In summary, within the sensitivity of this experiment, [^{3}H]NMS and 77-LH-28-1 competed for binding to the wild-type M_1 mAChR. In contrast, they bound simultaneously to the Tyr82 Ala mutant to form a ternary complex with a negative cooperativity of about 0.05. The aromatic side chain of Tyr82 may mediate interactions between the binding sites for the two ligands in the wild-type receptor, and its removal changes the mechanism of interaction between them (Lebon *et al.*, 2009).

Future perspectives: challenges for ligand binding assays

In the forgoing, we have addressed a limited agenda, focusing on equilibrium binding assays under a restricted set of conditions. Such assays are biased towards the discovery of molecules that compete with the tracer ligand, although allosteric interactions may also be detected. In the concluding section, we briefly outline some areas in which further developments are desirable.

The tracer ligands used in pharmacology are often antagonists. We have not discussed the increasingly important subject of allosteric modulation of agonist binding. Allosteric interplay between synthetic ligands and the orthosteric transmitter binding sites on receptors is a rich source of novel leads for drug development (Conn *et al.*, 2009). Because the binding sites for allosteric ligands are structurally distinct, they often support high selectivity that cannot be achieved at the evolutionarily conserved orthosteric site. Therefore, it is important to learn how to detect allosteric interactions with agonists in binding assays, and to understand their potential implications for drug screening.

Most ligand binding studies are carried out on membranes at or near room temperature. They do not distinguish between the enthalpy and the entropy of binding, both of which are subsumed into the expression $\Delta G^\circ = -RT\ln K$ for the standard Gibbs free energy. Therefore, an important motivation for binding studies at different temperatures is to resolve the ligand binding energy into its enthalpic and entropic elements. In straightforward cases, this is achieved by performing experiments at different temperatures, analyzing the variation of the binding constants using the van't Hoff relationship, $\ln K = -\Delta H^\circ/RT + \Delta S^\circ/R$.

Interestingly, for some GPCRs, as well as ligand-gated ion channels, thermodynamic measurements differentiate agonists from antagonists. For instance, agonist binding to β-adrenergic receptors is primarily enthalpy driven (Weiland *et al.*, 1979), while antagonist binding has a greater entropic component. The converse is true for adenosine A_1 and A_{2A} receptors (Borea *et al.*, 2000). At the human adenosine A_3 receptor (Merighi *et al.*, 2002) and A_{2B} receptor (Gessi *et al.*, 2008), data demonstrated that agonists were entropy driven whereas antagonist binding was dependent on entropy and enthalpy. It is notable that, in important instances, the optimization of affinity and selectivity evolved during drug development has come from the enthalpic rather than the entropic component of the binding energy (Raffa 1999; Freire, 2008). This arose from the introduction of strong, specific directional bonds such as hydrogen bonds and dispersion interactions without countervailing restrictions of conformational flexibility in the bound state or extra desolvation penalties. Such data have added an important extra dimension to ligand comparisons, and are increasingly viewed as important for optimization (Ruben *et al.*, 2006). It remains an outstanding intellectual challenge to calculate ligand affinities from knowledge of the structure of receptor molecules (Davis *et al.*, 2008).

Thermodynamic studies of drug–receptor interactions require the careful standardization of reaction, particularly buffer, conditions, if meaningful comparisons between different data sets are to be possible, especially when they originate from different laboratories. This has been something of a Cinderella's kitchen. Different groups have their favourite buffer recipes, which are often followed out of custom.

Clearly, if temperature is to be varied, it is advisable to choose a buffer whose pK is relatively temperature insensitive, and to titrate the pH of the buffer at the working point. This disfavours Tris–Cl, whose pK decreases by 0.028/°C. 'Good' buffers, such as HEPES, are less affected. Phosphate shows little temperature sensitivity, but is not compatible with divalent cations. Tris also has chelating activity for multivalent cations, and may cause a physical perturbation of the phospholipid bilayer (Mou *et al.*, 1994).

Receptor molecules contain ionizable groups. These may lie within the binding site or be allosterically linked to it. Ligands, such as tertiary amines, may also contain ionizable moieties (Barlow and Winter, 1981). Thus, pH variations may strongly affect ligand affinities. This must be considered at the outset of experiments, and standard conditions established.

Ionic strength also modulates receptor–ligand interactions. The binding of cationic amines to receptors which is mediated by anionic residues, such as the transmembrane helix 3 aspartic acid in aminergic GPCRs, is typically screened by increasing ionic strength (Birdsall *et al.*, 1979), but the effects may be quite different for selective or allosteric ligands acting at a distinct site (Pedder *et al.*, 1991), leading to large perturbations of structure–binding relationships. Interestingly, a sodium ion stabilizes the C-terminus of a short α-helical segment in the second extracellular loop of the turkey β_1 adrenergic receptor, revealed in the X-ray structure (Warne *et al.*, 2008). This may regulate the docking kinetics of ligands in transit to the binding site. The hydration of the ligand and of the receptor binding sites will also be changed by the formation of the receptor–ligand complex (Hulme *et al.*, 2006). This can provide a large element of the free energy change that drives binding, and may also be affected by the pH and ionic composition of the medium.

Ions can have specific effects on receptor binding and function. Selective sodium inhibition of the binding of α_2 adrenoceptor, mu opioid receptor and D2 dopamine receptor agonists, and promotion of the binding of opioid inverse agonists is thought to be mediated by an allosteric interaction of Na^+ with the 'polar pocket' residues clustered around a conserved aspartic acid residue in transmembrane helix 2,

reducing the affinity of the agonist–receptor complex for the G protein (Tian and Deth, 1993). In contrast, Mg^{2+} ions have the opposite effect on many GPCRs, promoting the formation of a high-affinity agonist–receptor–G protein complex, an instance of positive cooperativity that stabilizes the transition state of G protein activation (Zhang *et al.*, 2004). Usually, Mg^{2+} concentrations of the order of 1 mM are required: 10 mM Mg^{2+} may be added to the binding buffer to promote maximum agonist–GPCR–G protein interactions. Sometimes, 1 mM Mn^{2+} is used. This has a more potent effect, but creates a non-physiological form of the agonist–receptor–G protein complex.

Finally, it is impossible, in a membrane suspension, to reproduce the cellular environment of receptors vectorially inserted into the plasma membrane of a living cell, subject to large ionic and potential gradients. Nonetheless, it is becoming increasingly clear that transmembrane gradients may have an important effect on the function of GPCRs, as well ligand-gated ion channels (Ben Chaim *et al.*, 2006; Liu *et al.* 2009). It may become possible, in the near future, to address these issues by observing the binding of single ligand molecules to receptors embedded in lipid films, or in liposomes, using fluorescence techniques.

Acknowledgement

Edward C. Hulme is supported by the Medical Research Council, UK (Grant-in-Aid: U1175.03.003.00008.01).

References

Alexander SPH, Mathie A, Peters JA (2008). *Guide to Receptors and Channels (GRAC)*, 3rd edn (2008 revision). *Br J Pharmacol* **153** (Suppl. 2): S1–S209.

Avlani VA, McLoughlin DJ, Sexton PM, Christopoulos A (2008). The impact of orthosteric radioligand depletion on the quantification of allosteric modulator interactions. *J Pharmacol Exp Ther* **325**: 927–934.

Barlow RB, Winter EA (1981). Affinities of the protonated and non-protonated forms of hyoscine and hyoscine *n*-oxide for muscarinic receptors of the guinea-pig ileum and a comparison of their size in solution with that of atropine. *Br J Pharmacol* **72**: 657–664.

Ben Chaim Y, Chanda B, Dascal N, Bezanilla F, Parnas I, Parnas H (2006). Movement of 'gating charge' is coupled to ligand binding in a G-protein-coupled receptor. *Nature* **444**: 106–109.

Birdsall NJ, Lazareno S (2005). Allosterism at muscarinic receptors: ligands and mechanisms. *Mini Rev Med Chem* **5**: 523–543.

Birdsall NJ, Burgen AS, Hulme EC, Wells JW (1979). The effects of ions on the binding of agonists and antagonists to muscarinic receptors. *Br J Pharmacol* **67**: 371–377.

Borea PA, Dalpiaz A, Varani K, Gilli P, Gilli G (2000). Can thermodynamic measurements of receptor binding yield information on drug affinity and efficacy? *Biochem Pharmacol* **60**: 1549–1556.

Carter CM, Leighton-Davies JR, Charlton SJ (2007). Miniaturized receptor binding assays: complications arising from ligand depletion. *J Biomol Screen* **12**: 255–266.

Cheng Y, Prusoff WH (1973). Relationship between the inhibition constant (KI) and the concentration of inhibitor which causes 50 per cent inhibition (I_{50}) of an enzymatic reaction. *Biochem Pharmacol* **22**: 3099–3108.

Conn PJ, Christopoulos A, Lindsley CW (2009). Allosteric modulators of GPCRs: a novel approach for the treatment of CNS disorders. *Nat Rev Drug Discov* **8**: 41–54.

Copeland RA, Pompliano DL, Meek TD (2006). Drug-target residence time and its implications for lead optimization. *Nat Rev Drug Discov* **5**: 730–739.

Davis AM, St Gallay SA, Kleywegt GJ (2008). Limitations and lessons in the use of X-ray structural information in drug design. *Drug Discov Today* **13**: 831–841.

Dowling MR, Charlton SJ (2006). Quantifying the association and dissociation rates of unlabelled antagonists at the muscarinic M_3 receptor. *Br J Pharmacol* **148**: 927–937.

Fisher SK (1988). Recognition of muscarinic cholinergic receptors in human SK-N-SH neuroblastoma cells by quaternary and tertiary ligands is dependent upon temperature, cell integrity, and the presence of agonists. *Mol Pharmacol* **33**: 414–422.

Freire E (2008). Do enthalpy and entropy distinguish first in class from best in class? *Drug Discov Today* **13**: 869–874.

Gessi S, Fogli E, Sacchetto V, Varani K, Merighi S, Leung E *et al.* (2008). Thermodynamics of A2B adenosine receptor binding discriminates agonistic from antagonistic behaviour. *Biochem Pharmacol*. **75**: 562–569.

Glickman JF, Schmid A, Ferrand S (2008). Scintillation proximity assays in high-throughput screening. *Assay Drug Dev Technol* **6**: 433–455.

Goldstein A, Barrett RW (1987). Ligand dissociation constants from competition binding assays: errors associated with ligand depletion. *Mol Pharmacol* **31**: 603–609.

Heise CE, Sullivan SK, Crowe PD (2007). Scintillation proximity assay as a high-throughput method to identify slowly dissociating non-peptide ligand binding to the GnRH receptor. *J Biomol Screen* **12**: 235–239.

Hulme EC (1999). Analysis of binding data. In: Keen M (ed.). *Methods in Molecular Biology: Receptor Binding Techniques*. Humana Press Inc: Totowa, NJ, pp. 139–184.

Hulme EC, Birdsall NJM (1992). Strategy and tactics in receptor-binding studies. In: Hulme EC (ed.). *Receptor–Ligand Interactions – A Practical Approach*. IRL Press: Oxford, pp. 63–176..

Hulme EC, Soper AK, McLain SE, Finney JL (2006). The hydration of the neurotransmitter acetylcholine in aqueous solution. *Biophys J* **91**: 2371–2380.

Lazareno S (1998). Quantification of receptor interactions using binding methods. In: Leff P (ed.). *Receptor-based Drug Design*. Marcel Dekker Press: New York, NY, pp. 49–78.

Lazareno S, Birdsall NJM (1995). Detection, quantitation, and verification of allosteric interactions of agents with labelled and unlabeled ligands at G protein-coupled receptors: interactions of strychnine and acetylcholine at muscarinic receptors. *Mol Pharmacol* **48**: 362–378.

Lazareno S, Birdsall NJ (2000). Effects of contamination on radioligand binding parameters. *Trends Pharmacol Sci* **21**: 57–60.

Lebon G, Langmead CJ, Tehan BG, Hulme EC (2009). Mutagenic mapping suggests a novel binding mode for selective agonists of M_1 muscarinic acetylcholine receptors. *Mol Pharmacol* **75**: 331–341.

Liu QH, Zheng YM, Korde AS, Yadav VR, Rathore R, Wess J *et al.* (2009). Membrane depolarization causes a direct activation of G protein-coupled receptors leading to local Ca^{2+} release in smooth muscle. *Proc Natl Acad Sci USA* **106**: 11418–11423.

May LT, Leach K, Sexton PM, Christopoulos A (2007). Allosteric modulation of G protein-coupled receptors. *Annu Rev Pharmacol Toxicol* **47**: 1–51.

Merighi S, Varani K, Gessi S, Klotz KN, Leung E, Baraldi PG *et al.* (2002). Binding thermodynamics at the human A(3) adenosine receptor. *Biochem Pharmacol*. **63**: 157–161.

Motulsky HJ, Mahan LC (1984). The kinetics of competitive radioligand binding predicted by the law of mass action. *Mol Pharmacol* **25**: 1–9.

Mou J, Yang J, Shao Z (1994). Tris(hydroxymethyl)aminomethane (C4H11NO3) induced a ripple phase in supported unilamellar phospholipid bilayers. *Biochemistry* **33**: 4439–4443.

Pedder EK, Eveleigh P, Poyner D, Hulme EC, Birdsall NJ (1991). Modulation of the structure–binding relationships of antagonists for muscarinic acetylcholine receptor subtypes. *Br J Pharmacol* **103**: 1561–1567.

Raffa RB (1999). (Extra)thermodynamics of the drug–receptor interaction. *Life Sci* **65**: 967–980.

Rovati GE (1998). Ligand-binding studies: old beliefs and new strategies. *Trends Pharmacol Sci* **19**: 365–369.

Ruben AJ, Kiso Y, Freire E (2006). Overcoming roadblocks in lead optimization: a thermodynamic perspective. *Chem Biol Drug Des* **67**: 2–4.

Schumacher C, Von TV (1994). Practical instructions for radioactively labelled ligand receptor binding studies. *Anal Biochem* **222**: 262–269.

Sharif NA, Williams GW, DeSantis LM (1995). Affinities of muscarinic drugs for [3H]*N*-methylscopolamine (NMS) and [3H]oxotremorine (OXO) binding to a mixture of M_1–M_4 muscarinic receptors: use of NMS/OXO-M ratios to group compounds into potential agonist, partial agonist, and antagonist classes. *Neurochem Res* **20**: 669–674.

Stockton JM, Birdsall NJ, Burgen AS, Hulme EC (1983). Modification of the binding properties of muscarinic receptors by gallamine. *Mol Pharmacol* **23**: 551–557.

Sullivan SK, Hoare SR, Fleck BA, Zhu YF, Heise CE, Struthers RS *et al.* (2006). Kinetics of nonpeptide antagonist binding to the human gonadotropin-releasing hormone receptor: implications for structure–activity relationships and insurmountable antagonism. *Biochem Pharmacol* **72**: 838–849.

Sum CS, Pyo N, Wells JW (2001). Apparent capacity of cardiac muscarinic receptors for different radiolabeled antagonists. *Biochem Pharmacol* **62**: 829–851.

Swillens S (1995). Interpretation of binding curves obtained with high receptor concentrations: practical aid for computer analysis. *Mol Pharmacol* **47**: 1197–1203.

Swinney DC (2009). The role of binding kinetics in therapeutically useful drug action. *Curr Opin Drug Discov Devel* **12**: 31–39.

Tian WN, Deth RC (1993). Precoupling of Gi/G(o)-linked receptors and its allosteric regulation by monovalent cations. *Life Sci* **52**: 1899–1907.

Wang ZX, Jiang RF (1996). A novel two-site binding equation presented in terms of the total ligand concentration. *FEBS Lett* **392**: 245–249.

Warne T, Serrano-Vega MJ, Baker JG, Moukhametzianov R, Edwards PC, Henderson R *et al.* (2008). Structure of a beta1-adrenergic G-protein-coupled receptor. *Nature* **454**: 486–491.

Weiland GA, Minneman KP, Molinoff PB (1979). Fundamental difference between the molecular interactions of agonists and antagonists with the beta-adrenergic receptor. *Nature* **281**: 114–117.

Wells JW, Birdsall NJ, Burgen AS, Hulme EC (1980). Competitive binding studies with multiple sites. Effects arising from depletion of the free radioligand. *Biochim Biophys Acta* **632**: 464–469.

Zhang Q, Okamura M, Guo ZD, Niwa S, Haga T (2004). Effects of partial agonists and Mg^{2+} ions on the interaction of M_2 muscarinic acetylcholine receptor and G protein Galpha I1 subunit in the M_2-Galpha I1 fusion protein. *J Biochem* **135**: 589–596.